Japan Geoscience Union Meeting 2013
(May 19-24 2013 at Makuhari, Chiba, Japan)

SSS28-01 Room:303 Time:May 22 16:15-16:30

An arithmetic geometrical approach for modeling of seismic activity

Hiroyuki Fujiwara[1*]

[1]NIED

Earthquake occurs in a discrete manner in time and space. Except for the main shock-aftershock sequences, earthquakes that seem to be individually independent. However, when viewed as a whole, we find that there are laws, for example, G-R law, that govern the entire earthquakes that seem to be individually independent.

A similar phenomenon can be observed also in the world of "number". The most basic example is the distribution of the prime numbers in integers. The presence of interesting relationships, for example, the reciprocity law of quadratic residue, has been found in prime numbers that seem to be individually independent. Class field theory as a theoretical system relates to the structure of the number has been established. In addition, a lot of knowledge is going to be achieved in recent years by the development of arithmetic geometry that regards "number" as geometric objects. Arithmetic geometry was developed by applying the theory of scheme to "number", which was developed in algebraic geometry aimed to study algebraic varieties consisting of zeros of polynomials. Arithmetic geometry have revealed interesting laws that govern the world of the "number".

We consider the correspondence as follows to the world of "number" and "earthquake" that seem to be completely independent. Let p_i be the i-th prime and take appearance interval of prime, p_i-p_{i-1}, as index of i-th prime. Let e_i be the i-th earthquake, $T(e_i)$ be occurrence time of the i-th earthquake, and $M_o(e_i)$ be moment of the i-th earthquake. We assume that the following equations hold.

$T(e_i)=p_i$,

$\log(M_o(e_i))=p_i-p_{i-1}$

By performing numerical experiments, we have found that the characteristics of this correspondence are similar to the G-R law. We call the model obtained by this correspondence as "arithmetical seismic activity model".

Based on these considerations, we can regard the "arithmetical seismic activity model" as an object of the scheme theory. By using knowledge from the arithmetic geometry, it is expected to obtain knowledge about laws that control seismic activity. We have an image of earthquakes that fracture starts from a point in space that does not have infinite special boundary conditions and expand gradually to the destruction of the entire area. Although it is believed that the boundary conditions more realistic for the physical model, we expect to be able to handle them by considering to limit or to extend the "number" and those are objects of the scheme theory. By using the "arithmetical seismic activity model", the unresolved issue on the math as "the twin primes exist infinitely" is replaced by the problem of the nature of the seismic activity, such that the smallest earthquakes occur infinitely.

Keywords: prime, arithmetic geometry, Gutenberg-Richter relation, earthquake

Japan Geoscience Union Meeting 2013
(May 19-24 2013 at Makuhari, Chiba, Japan)

SSS28-02 Room:303 Time:May 22 16:30-16:45

Development of an epicenter estimation method using 3D polarity and its application to dynamic triggering events

Takahiko Uchide[1*]

[1]Disaster Prevention Research Institute, Kyoto University

Recently based on the development of seismic observations and computational resources, many methods to locate earthquakes with unclear P and S onset, such as low-frequency earthquakes and dynamic triggering earthquakes, have been proposed [e.g., Obara, 2002; Kao et al., 2005; Shelly et al., 2007].

Here I show a new method to estimate epicenters using the polarities of seismograms. The basic idea is as follows: First, we detect rectilinear signal from seismograms; then assuming such rectilinear waveforms are P waves and the polarization direction is same as the back azimuth, we estimate epicenters directed by multiple stations. This kind of strategy is often used to confirm hypocenter determinations with few stations. This study carries out this procedure automatically. The test field of this study is Hida region, Central Japan. The goal of this paper is so far to detect more events dynamically triggered by the 2011 Tohoku earthquake than those detected by manual process [Miyazawa, 2011].

I apply a polarization analysis method using analytic signal (its real and imaginary parts are an original signal and its Hilbert transform, respectively) of both horizontal and vertical components [Vidale, 1986]. We construct a variance-covariance matrix $\boldsymbol{C}(t)$ of the analytic signal at each time. Its eigenvector corresponding to the largest eigenvalue represents the polarization direction. The use of the moving average of data will stabilize the analysis. The strength of the polarization is represented by $P_s = 1 - (a_2 + a_3)/a_1$, where $a_1 > a_2 > a_3$ are the eigenvalues of $\boldsymbol{C}(t)$. If the polarization direct is downward, we change it to an upward one by changing the sign of dip angle and taking 180 degrees opposite of the azimuth.

In a realistic case, the polarization direction and back azimuth are not exactly same, because (1) the horizontal heterogeneity of seismic velocity structure and (2) the misorientation of seismometers. Those directions also differs, when (3) other phases such as S waves are analyzed. In case of (3), it is less probable that multiple stations indicate the same point. To check the effect of (1) and (2) quantitatively, I calculate the differences between the back azimuth and the polarization direction of seismograms for 0.5 s from P arrivals, from the phase information in the JMA unified earthquake catalog, from earthquakes in Hida region. At most of stations, the average and the standard deviation of them are within 5 degrees and 5 to 10 degrees, respectively, though at some stations the average is much larger, probably due to the misorientation of seismometers.

Based on the time history of the polarities, epicenters are searched by a grid-search manner, taking account of (a) travel time of P waves from a grid to stations, (b) difference between the polarization direction and azimuths from stations to a grid, and (c) the strength of the polarity P_s. I construct an evaluation function to search for an epicenter location and origin time.

This method is applied to single M2-class earthquakes in the Hida region using velocity seismograms from Hi-net and DPRI seismic network. The data is high-pass filtered at 4 Hz. The epicenters determined by my method are close to those of JMA unified catalog. When I analyze an earthquake outside of the network, ghost errors are seen.

Finally I apply this method to seismic data in the Hida region during seismic waves from the 2011 Tohoku earthquake are passing. The velocity seismograms are high-pass filtered at 4 Hz. Many events are detected. Some of them correspond to events detected by Miyazawa [2011], but some of them are not in his catalog.

This study will improve the catalog of dynamic triggering earthquakes and promotes the dynamic triggering studies. Moreover this method will contribute to other type of seismological studies, such as automatic data processing and structure studies.

Keywords: Epicenter determination method, 3D polarity of motion, Hida, Dynamic triggering of earthquakes, the 2011 Tohoku earthquake

Japan Geoscience Union Meeting 2013
(May 19-24 2013 at Makuhari, Chiba, Japan)

SSS28-03 Room:303 Time:May 22 16:45-17:00

Theoretical background of back-projection imaging and its relation to time-reversal and inverse solutions

Yukitoshi Fukahata[1*], Yuji Yagi[2], RIVERA, Luis[3]

[1]DPRI, Kyoto University, [2]Life and Environ. Sci., Univ. Tsukuba, [3]EOST, University of Strasbourg

The back-projection (BP) method has become a popular tool to image the rupture process of large earthquakes since the success of Ishii et al. (2005), while it has not been clear what the BP image represents physically. We clarified the theoretical background of the back-projection (BP) imaging and related it to classical inverse solutions via the hybrid back-projection (HBP) imaging (Yagi et al., 2012). In the HBP method, which is mathematically almost equivalent to the time-reversal imaging, cross correlations of observed waveforms with the corresponding Green's functions are calculated. The key condition for BP to work well is that the Green's function is sufficiently closer to the delta function after stacking. Then, we found that the BP image represents the slip motion on the fault, and approximately equals to the least squares solution. In HBP, instead of the Green's function in BP, the stacked auto-correlation function of the Green's function must be close to the delta function to obtain a fine image. Because the auto-correlation function is usually closer to the delta function than the original function, we can expect that HBP works better than BP, if we can reasonably estimate the Green's function. With another condition that the stacked cross-correlation function of the Green's functions for different source locations is small enough, the HBP image is approximately equal to the least squares solution. If these assumption are not satisfied, however, the HBP image corresponds to a damped least squares solution with an extremely large damping parameter, which is clearly inferior to usual inverse solutions. We show some simple examples of numerical computation to check the validity of the above mentioned conditions implicitly assumed in the BP and HBP methods.

Keywords: Back projection, Time reversal, Inversion, least squares solution

SSS28-04 Room:303 Time:May 22 17:00-17:15

Nondimensional Controlling Parameter about Inelastic Porosity Evolution Law and its Effect on Dynamic Earthquake Slip

Takehito Suzuki[1*], Teruo Yamashita[2]

[1]EPS, Univ. Tokyo, [2]ERI, Univ. Tokyo

In a series of our studies, we have studied effects of the interaction among effects of shear heating, fluid pressure and inelastic pore creation on dynamic fault slip and found two nondimensional controlling parameters Su and Su' about the interaction for one-dimensional (1-D) fault model. The parameter Su represents the relative dominance of the effect of inelastic pore creation on the fluid pressure change over that of shear heating, while Su' is associated with the dominance of fluid flow effect over the effect of shear heating. We have succeeded in explaining many aspects of dynamic earthquake slip behavior in a unified way on the basis of the parameters: for example, ordinary earthquakes and slow earthquakes are understood in terms of those parameters.

However, there is a problem in our modeling that we have assumed too simple form of inelastic porosity evolution; inelastic porosity change rate was assumed to be proportional to slip velocity. Porosity in natural faults is suggested to have an upper limit, phi$_{inf}$, by observational and experimental studies. The framework the authors have employed assumes that porosity change, phi, is negligibly smaller than the upper limit.

We introduce the third nondimensional parameter, Su^{ul}, to describe the effect of the upper limit of inelastic porosity. We neglect here fluid flow; that is, Su'=0. If we assume Su$>$1, fluid pressure decrease due to inelastic pore creation at an initial stage of slip reduces slip velocity. After the initial stage, two qualitatively different behaviors of slip appear. For some parameter ranges of Su and Su^{ul}, slip accelerates and the slip velocity approaches to a positive constant value. This behavior occurs because phi approximately approaches to phi$_{inf}$ and effect reducing the fluid pressure (and the slip velocity) due to pore creation vanishes. In this case, shear stress acting on a fault plane is completely released at the final stage due to thermal pressurization. On the other hand, for the other ranges, slip velocity approximately approaches to zero and the slip ceases spontaneously because phi is so small that the effect of phi$_{inf}$ does not appear. Both high speed slip and spontaneous slip cessation can be understood in a single framework in the present model.

We also found that two important governing porosities, phi$_1*$ and phi$_2*$, exist in the present model and succeeded in obtaining their analytical forms in terms of Su and Su^{ul}. The value phi$_f*$, defined as the value of normalized inelastic porosity phi$*$ after an infinitely long time, cannot take values between phi$_1*$ and unity at the stable state (situation where phi$*$ is unity represents phi equals to the upper limit) because if phi$*$ approaches to phi$_1*$, the slip accelerates and phi$_f*$ takes a value unity. The porosity phi$_1*$ can be regarded as the critical value distinguishing the system behavior, slip acceleration and spontaneous slip cessation. In addition, the value of phi$_f*$ cannot take values smaller than phi$_2*$, which is related to thermal energy generation. Observed porosity can be an indicator of thermal energy.

Keywords: heat, fluid pressure, inelastic porosity, high speed slip, spontaneous slip cessation

Japan Geoscience Union Meeting 2013
(May 19-24 2013 at Makuhari, Chiba, Japan)

SSS28-05 Room:303 Time:May 22 17:15-17:30

Development of extended BIEM and its application to earthquake dynamic rupture analysis in inhomogeneous media

Tetsuya Kusakabe[1*], Nobuki Kame[1]

[1]Earthquake Res. Inst., Univ. of Tokyo

The boundary integral equation method (BIEM) has been applied to the analysis of rupture propagation of non-planar faults in an unbounded homogeneous elastic medium. We have proposed an extended BIEM (XBIEM) that is applicable in an inhomogeneous bounded medium consisting of homogeneous sub-regions (Kame and Kusakabe, 2012). We have developed a preliminary code for mode III dynamic rupture propagation interacting with medium interfaces. The validation tests have been carried out by comparing the XBIEM results with the BIEM solution for simple problems of the wave propagation and the dynamic rupture in a homogeneous full-space with a planar interface. It was found out that the discretized interfaces worked well for both problems.

In the present paper, we additionally validated our numerical code for two specific cases: 1) wave propagation in a homogeneous media with a non-planar interface and 2) wave propagation in a bimaterial with a planar interface. For the first case, it was found out that non-planar interface worked quite well. For the second case, our numerical result showed a good agreement with Hirano's analytic solution (Hirano, private communication). In both cases, our numerical code worked well enough and we proceed to apply our code to a new type of problem: dynamic rupture propagation interacting with a medium interface.

Here we considered dynamic rupture propagation on a planar fault embedded normal to the planar interface of a bimaterial. Spontaneous rupture is allowed not only on the planar main fault but also on the interfacial fault and it is controlled by slip-weakening laws on them: their peak strength are separately chosen and its ratio zeta=tau^peak_main/tau^peak_interface is chosen as one of controlling parameters. Another parameter is eta chosen as a ratio of the shear wave velocities, eta=beta_+/beta_-. Simulations were conducted for hundreds of parameter sets of (eta, zeta). Our results showed two distinct rupture processes: a) one is to propagate rupture just on the prescribed fault, and b) another is to activate the subsidiary interfacial rupture, which finally results in arresting rupture on the main planar fault.

Two processes were found to be clearly divided by a line in the parameter plane (eta, zeta). With increasing zeta, rupture tends to stay on the main fault with less significant activation of subsidiary interfacial rupture and it agrees with our physical anticipation. With increasing eta from 0.7 to 1.3 (one means homogeneous), rupture process shifts from (a) to (b). This eta dependency is not easily understandable at this moment but it clearly showed a significant effect of inhomogeneous medium on arresting dynamic rupture.

Keywords: dynamic rupture, BIEM, bimaterial interface, simulation

Japan Geoscience Union Meeting 2013
(May 19-24 2013 at Makuhari, Chiba, Japan)

SSS28-06 Room:303 Time:May 22 17:30-17:45

3D dynamic rupture simulation of a subducting reverse fault and its branch fault

Shintaro Tamura[1*], Satoshi Ide[1]

[1]Univ. of Tokyo, EPS

The Mw 9.0 Tohoku-Oki earthquake hit the northeast Japan on March 11, 2011 generating huge strong motion and tsunami and the area with the largest slip amount was located near the Japan Trench. Exploring the dynamics of the Tohoku-Oki earthquake is important for understanding physics of mega-thrust earthquakes and estimating the probability of rupture extensions or tsunami geneses to prevent future disasters. We model a shallow dipping mega-thrust earthquake on a bi-material interface with a free surface by using a 3D finite element method to solve elastodynamic equations and a slip-weakening friction law on the fault plane. As a preliminary study, we simulate in the relatively simple situations with a planar fault and a homogeneous prestress. Reflected body waves from the free surface strongly affect the normal and shear stress on the fault, and both the normal and the shear stress decrease just after the rupture reaches the trench. The slip on the fault reflects at the trench and rapidly propagates downward at the P-wave velocity. This downward reflected slip is consistent with the west-northwest directivity of the Tohoku-Oki earthquake. Final slip distribution with largest slip at the trench is also consistent with some kinematic slip models. Deformation style of the free surface changes depending on the dip angle and material contrast. The amount of vertical motion of the hanging wall is larger for the case of more compliant hanging wall and much larger than that of the footwall. Our simulations suggest that the huge tsunami is generated due to large amount of the surface deformation which is enhanced in the wedge part of the compliant hanging wall.

Keywords: dynamic rupture modeling in a subduction zone, branch fault, plastic yielding, FEM

SSS28-07 Room:303 Time:May 22 17:45-18:00

Difference in the seismic rupture process between slow tsunami and megathrust earthquakes

Yuji Yagi[1*], Yuta Mitsui[2], Hayaki Ezaki[1]

[1]Life and Env. Sci., Univ. of Tsukuba, [2]Sci., Hokkaido Univ.

After the 2011 Tohoku earthquake, we know that huge co-seismic slip can occur at shallow part of subduction zone where slow tsunami earthquakes have been detected (e.g. the 1986 Meiji-Sanriku earthquake). To understand the nature of megahrust earthquakes as well as slow tsunami earthquakes, it is important to investigate the slip behavior in the area. We estimated the spatio-temporal slip-rate distribution of megathrust and slow tsunami earthquakes using a novel seismic source inversion method (Yagi and Fukahata, 2011, GJI) and a Hybrid Back-projection method (Yagi et al., 2012, EPSL), and then compared the observation results to simulation results. We inverted and projected the slip-rate function on fault for the 1992 Nicaragua slow tsunami earthquake, the 2006 Java slow tsunami earthquake, the 2010 Mentawai slow tsunami earthquake, and the 2011 Tohoku megathrust earthquake. In the case of slow tsunami earthquakes, we found a smooth and slow slip (~0.1m/s) that continued over 50 s near the trench, while pulse-like slip was detected in and around the main-shock hypocenter. In the case of the 2011 Tohoku megathrust earthquake, we also found a smooth and fast slip (~1.0 m/s) that continued over 80 s near the trench. The slow tsunami and megathrut earthquakes have a release of seismic energy in the downdip area that triggered smooth slip in the updip area. The difference of slip-rate between the analyzed slow tsunami earthquakes and Tohoku megathrust earthquake may suggest the existence of a non-linear rupture characteristic in the shallowest megathrust faults. Next, we performed dynamic rupture simulations using simplified fault models and the mechanism of thermal fluid pressurization. We found that small fluctuations of initial shear stress near the trench, within 1 MPa, lead to differences in seismic moment release greater than two orders of magnitude. Moderate slip events with trapezoidal source time functions appear to occupy a transition position, between shallow megathrust earthquakes, with surface rupture, and smaller ordinary earthquakes, without surface rupture. We interpret this result as representing the differences in interplate slip between shallow megathrust earthquakes, tsunami earthquakes, and ordinary earthquakes in the same region. The observation and numerical simulation results suggest that the dynamic frictional weakening in the shallower segment plays a crucial role in the interaction between the deeper and the shallower segments.

Keywords: Slow tsunami earthquake, Megathrust earthquake, The Tohoku earthquake, Slip-rate, Slow slip

Japan Geoscience Union Meeting 2013
(May 19-24 2013 at Makuhari, Chiba, Japan)

SSS28-08 Room:303 Time:May 23 09:00-09:15

Fault modeling of the foreshocks of the 2011 Tohoku-oki earthquake based on near-field tsunami observation

Tatsuya Kubota[1*], Ryota Hino[1], Takeshi Iinuma[2], Yoshihiro Ito[1], Yusaku Ohta[1], Syuichi Suzuki[1], Daisuke Inazu[3], Tatsuhiko Saito[3], Yoshiyuki Kaneda[4]

[1]Graduate School of Science, Tohoku University, [2]International Research Institute of Disaster Science, [3]National Research Institute fo Earth Science and Disaster Prevention, [4]Japan Agency for Marine-Earth Science and Technology

We calculated the fault slip distribution of two large (Mw 7.3 on March 9 and Mw 6.5 on March 10) foreshocks of the 2011 Tohoku-Oki mainshock (Mw 9.0 on March 11) by inverting tsunami waveforms recorded by ocean bottom pressure gauges (OBPs) that had been deployed around the source area of the mainshock. These two foreshocks are the two largest foreshocks of the Mw9.0 mainshock. Both tsunami and coseismic vertical displacement of the seafloor were recorded clearly by OBPs. For the Mw 7.3 foreshock, the recorded tsunami amplitude and seafloor vertical displacement were up to 15 and 10 cm, respectively. During the Mw 6.5 foreshock, the vertical movement of 4 cm uplift was recorded at one of the OBP stations, and the tsunami with an amplitude of about 3 cm was recorded at several stations. In the tsunami waveform inversion for the both foreshocks, we use the same fault geometry based on Ito et al. (2005). As a first step of our analyses, we estimated the initial water surface height distribution through the inversion. The result is consistent with the pure reverse-fault type focal mechanism for both foreshocks. The results indicate that the main slip area of the Mw 7.3 foreshock is 40 km in length and 40 km in width and is located to the northwest of its epicenter. The maximum slip and the magnitude are estimated to be 1.0 m and Mw 7.3, respectively. The results indicate that the Mw 6.5 foreshock occurred about 20 km south of the epicenter of the Mw 7.3 foreshock and that the main slip area is 20 km in length and 40 km in width and is situated to the west of its epicenter. The maximum slip and magnitude are estimated to be 0.2 m and Mw 6.6. The calculated main slip area of the Mw 6.5 foreshock is located immediately south of the Mw 7.3 foreshock and is sandwiched between the epicenters of the Mw 7.3 foreshock and the mainshock. This indicates that the aseismic rupture propagated southwards sequentially. The postseismic slip of the Mw 7.3 foreshock likely caused aftershocks, which led to the second largest Mw6.5 foreshock. There were more aftershocks following the Mw 6.5 foreshock than Mw 7.3 foreshock. It is likely that this swarm of aftershocks triggered the initial rupture of the mainshock. The comparison between the tsunami sources of an M 7.0 earthquake off Miyagi in 1981 and the Mw 7.3 foreshock indicates that the Mw7.3 foreshock ruptured the same area of the 1981 event or that the area partially contained the rupture area of the 1981 earthquake.

Keywords: The 2011 off the Pacific coast of Tohoku earthquake, Foreshocks, Tsunami

SSS28-09 Room:303 Time:May 23 09:15-09:30

Rupture Process of The 2011 Tohoku-Oki Earthquake Inferred by a Waveform Inversion Using 3D Green's Tensor Synthetics

Taro Okamoto[1*], Hiroshi Takenaka[2], Tatsuhiko Hara[3], Takeshi Nakamura[4], Takayuki Aoki[5]

[1]Dept. Earth Planet. Sci., Tokyo Institute of Technology, [2]Dept. Earth Planet. Sci., Kyushu University, [3]IISEE, Building Research Institute, [4]JAMSTEC, [5]GSIC, Tokyo Institute of Technology

The March 11, 2011 Tohoku-Oki earthquake (GCMT Mw9.1) generated strong ground motions and large tsunamis, and caused devastating damages in the northeastern Japan. Estimating the rupture process of this event is very important for understanding the geophysical condition of the generation of megathurust earthquakes and the mechanism of the excitation of the large tsunamis.

We present the rupture process analysis of the 2011 Tohoku-Oki earthquake by using a non-linear full-waveform inversion method in which the teleseismic and the strong motion seismograms are jointly used. We incorporate the effect of the near-source laterally heterogeneous structure on the synthetic Green's tensor waveforms because the solution can be erroneous one if the effect is not considered (e.g., if only a flat layered structure is used) [1]. For the teleseismic P-wave synthetics we use a 2.5-dimensional finite-difference method [2]. For the strong motion synthetics we use a full three-dimensional finite-difference method that incorporates topography, oceanic water layer, three-dimensional heterogeneity and attenuation. Our simulation is accelerated by the use of hundreds of GPUs used in parallel [3]. We use a GPU supercomputer, the TSUBAME-2.0 in Tokyo Institute of Technology.

As a preliminary analysis we computed Green's tensor synthetic waveforms for 31 teleseismic and 15 strong motion components. We used 640 GPUs of the TSUBAME supercomputer for the calculation of each strong motion synthetics. The inferred slip distribution has large slips near and around the JMA epicenter and has relatively less slips near the trench: the major rupture apparently migrate toward the north of the epicenter and the maximum slip is about 40 m. We will present results by incorporating more strong ground motion records and discuss the effect of the choice of the Green's tensor waveforms on the solutions.

[1] Okamoto and Takenaka, Earth Planets Space, 61, e17-e20, 2009.
[2] Takenaka and Okamoto, in Seismic Waves, Research and Analysis, ed. Kanao Masaki, Intech, 2012.
[3] Okamoto et al, in GPU Solutions to Multi-scale Problems in Science and Engineering, ed. D.A. Yuen et al., Springer, 2013.

Keywords: 2011 Tohoku-Oki earthquake, rupture process, 3D finite-difference method

SSS28-10 Room:303 Time:May 23 09:30-09:45

2011 Tohoku earthquake: Unified source model and its rupture process

Yusuke Yokota[1], Kazuki Koketsu[1*], Yushiro Fujii[2]

[1]Earthquake Research Institute, University of Tokyo, [2]International Institute of Seismology and Earthquake Engineering, Building Research Institute

The devastating 2011 Tohoku earthquake was observed by dense networks of strong motion, teleseismic, geodetic, and tsunami. We performed checkerboard resolution tests for assessing the resolving power of the datasets obtained by the networks. From the results, we found that the individual datasets had only limited resolutions. In order to overcome these limitations, Koketsu *et al.* (2011) constructed the first version of the unified source model through a triple joint inversion of the teleseismic, strong motion, and geodetic datasets. Yokota *et al.* (2011) next performed a quadruple joint inversion of all the four datasets to determine the 1.5th version of the unified source model.

Although the above inversions were performed using one-dimensional Green's functions, we constructed the second version of this unified source model inferred taking three-dimensional (3-D) velocity structures into consideration. To achieve this, we calculated the 3-D Green's functions using the finite element method. We first inverted each of the datasets separately, and then performed a triple joint inversion of the strong motion, geodetic, and tsunami datasets for the second version of the unified source model. The teleseismic dataset was excluded, because the checkerboard tests had shown its low resolving power.

The total seismic moment in the second version was calculated to be 4.2 x 10^{22} Nm, which yielded M_W 9.0. This model revealed that the first rupture expanded at a slow speed of 2.0 km/s to the Japan Trench after small rupture in the initial 40 s. The second rupture began 20 s later at the slowest speed of 1.7 km/s and became dominant with the largest slip of 36 m. The third rupture then played the leading role, propagating southward at a speed of 2.5 km/s. The slow rupture speed and first rupture to the Japan Trench can explain the features of the disaster by the earthquake.

Keywords: 2011 Tohoku earthquake, unified source model, rupture process

Japan Geoscience Union Meeting 2013
(May 19-24 2013 at Makuhari, Chiba, Japan)

SSS28-11 Room:303 Time:May 23 09:45-10:00

Similarities and differences of the 1952 and 2003 Tokachi-oki earthquakes

Hiroaki Kobayashi[1*], Kazuki Koketsu[1], Hiroe Miyake[1], Hiroo Kanamori[2]

[1]ERI, Univ. Tokyo, [2]Caltech

Along the Kuril Trench off the Pacific coast of Hokkaido, many destructive earthquakes have occurred. Among those, the 1952 Tokachi-oki earthquake (41.706^{o}N, 144.151^{o}E, depth: 52 km) and the 2003 Tokachi-oki earthquake (41.779^{o}N, 144.079^{o}E, depth: 45 km) were very close to each other and their magnitudes (M_{JMA} 8.2 and M_{JMA} 8.0) were also close to each other. Therefore, it is highly possible that these two earthquakes were characteristic plate-boundary earthquakes.

The source process of the 1952 earthquake was analyzed using strong-motion data (Yamanaka and Kikuchi, 2003) and tsunami data (Hirata *et al*., 2003; Satake *et al*., 2006). However, the slip distributions obtained by those studies were different from each other, because many strong-motion seismograms went off scale after the S-wave arrival so that sufficient data length was not available for the strong-motion data.

In this study, we performed joint inversions of teleseismic data which were recorded with enough lengths and strong-motion data to analyze the whole rupture process of the 1952 earthquake. We also analyzed the 2003 earthquake with the same methods to examine the differences and similarities of these two earthquakes.

For the dataset of the 1952 earthquake, we collected the copies of seismograms which were recorded by historical seismographs, and digitized them. For the dataset of the 2003 earthquake, we used teleseismic data from IRIS-DMC and strong-motion data from K-NET. When we selected the stations, we took care to include the stations which are identical to, or nearby, those of the 1952 earthquake.

We first compared the datasets of the two earthquakes. The results revealed that the 1952 earthquake was composed of two large events and the data from the first event look similar to the ones of the 2003 earthquake. In addition, the initial parts of data suggest that the 1952 earthquake was preceded by a small event.

Secondly, we performed joint inversions of the teleseismic and strong-motion data. The results showed that the 1952 earthquake was composed of two large events as shown in the above comparison. The rupture first propagated to the western part and then to the eastern part. The moment rate function of the western event was similar to the one of the 2003 earthquake and their rupture areas almost overlapped with each other.

In summary, the western event of the 1952 earthquake and the 2003 earthquake are characteristic great earthquakes, but the eastern event and the small event are specific only to the 1952 earthquake.

Keywords: source process, inversion, the 1952 Tokachi-oki earthquake, the 2003 Tokachi-oki earthquake, characteristic earthquake

Japan Geoscience Union Meeting 2013
(May 19-24 2013 at Makuhari, Chiba, Japan)

SSS28-12 Room:303 Time:May 23 10:00-10:15

Rupture process of the 2004 Sumatra earthquake using teleseismic body waves

Masahiro Yoshimoto[1*], Yoshiko Yamanaka[1]

[1]Environmental Studies, Nagoya Univ

The 2004 Sumatra earthquake was one of the largest earthquakes in recorded history, and had a ~1500 km long rupture of more than 500 seconds duration. To describe the whole rupture process of this earthquake, records of at least 500 seconds in duration were required for analysis. However, it is difficult to compute later phases using traditional rupture process analysis based on ray theory, which often uses the duration of analysis before the arrival of the later phases. In addition, such methods never compute a long period phase like a W phase. Although Ammon et al., (2005) inverted the rupture process using the Spectral Element Method which can compute the phases discussed above, they used body and surface waves at slightly long period range from 20 to 2000 seconds.

This study analyzes the rupture process of this earthquake using the Green's functions calculated by the Direct Solution Method (DSM). The Green's functions were computed up to 1 Hz for IASP91 model (Kennett and Engdahl, 1991) using the DSM software developed by Dr.Takeuchi (http://www.eri.u-tokyo.ac.jp/takeuchi/software/). The slip distributions were also determined using the waveform inversion scheme presented in Kikuchi et al. (2003).

The main results of waveform inversion are as follows: the moment magnitude, Mw, was determined to be 9.1; the source duration was 500 seconds; and the rupture velocity was 2.5-3.0 km/s. The synthetic seismograms matched well with the observations including the later phases and W phase. The largest slip area was estimated to be located from south west to west of the Sumatra islands, the second and third largest slip areas were estimated to be around the Nicobar islands, but almost no slip was found around the Andaman region.

Japan Geoscience Union Meeting 2013
(May 19-24 2013 at Makuhari, Chiba, Japan)

SSS28-13 Room:303 Time:May 23 10:15-10:30

Short recurrence intervals of repeating earthquakes in the Tonga subduction zone

Shimon Abe[1*], Satoshi Ide[1]

[1]Dept. EPS, Univ. Tokyo

The Tonga subduction zone is characterized by high seismicity and fast convergence rates exceeding 20 cm/year with a wide variation along the trench. We searched repeating earthquakes in this region and identified several sequences.

We selected 1399 M $>$ 5 events with the depth shallower than 60 km occurred from 1991 to 2011 in the ANSS global earthquake catalog. For all events, broadband seismograms at about 27 stations were downloaded from IRIS DMC, and bandpass filtered in 0.02 - 4Hz. For each pair of two events, we computed a cross-correlation function between vertical seismograms recorded at the station CTAO, Australia, for 800 s time windows around the theoretical S arrival times. We consider two events are repeating when the maximum of the cross-correlation function is larger than 0.9. Through this procedure and manual inspection of recurrence intervals, we identified 45 repeating earthquakes in 11 sequences. Almost all events have a low-angle thrust mechanism and for most sequences, the difference of relative S arrival times between stations are less than 0.5 s, suggesting the proximity of source regions.

The recurrence intervals of these events are very short despite their large size. For example, five M6 earthquakes occurred in 1993-2011, with the average recurrence interval of about 4.3 years. After the normalization of recurrence intervals using the scaling law of Nadeau and Johnson (1998), we found that the recurrence intervals are yet short, compared with those estimated in other regions such as northeastern Japan subduction zone and Parkfield, California. This difference can be explained by the different convergence rates.

Keywords: repeating earthquake, Tonga subduction zone

Japan Geoscience Union Meeting 2013
(May 19-24 2013 at Makuhari, Chiba, Japan)

SSS28-14 Room:303 Time:May 23 10:30-10:45

Earthquake depth estimations in the Po Plain (North Italy) using teleseismic data: influence on stress drop.

Jean Letort[1*], Massa Marco[3], Cotton Fabrice[1], Guilbert Jocelyn[2], Drouet Stephane[1], Pacor Francesca[3], Traversa Paola[4]

[1]ISTerre Universite de Grenoble 1, CNRS, F-38041 Grenoble, France., [2]CEA/DAM/DIF, F-91297 Arpajon Cedex, France., [3]Instituto Nazionale di Geofisica e Vulcanologia, Milano, Italy., [4]EDF, Aix en Provence, France

On May 2012, the central part of the Padano-Emiliana Plain (North Italy), has been shocked by a dramatic sequence of earthquakes, with higest Mw 6.0. These events were very shallow (~ 5-10 km) with low stress drops and large ground-motions amplitude have been observed in the fault area. On the opposite, on the last 25th and 27th January other two deeper moderate earthquakes (either with Mw 4.9) occurred in the same area (south of Parma). These two events made very few damages and no victims, but have been felt also far from the source, which could be explained by their important focal depths (33 and 65 km respectively). Hence, a study of depth influence on seismic properties is of great interest. However, Po plain is a very complex area, the largest alluvial basin of northern Italy, characterized by anomalous propagation dues to the variable thickness of quaternary alluvium and with complex Moho discontinuities (Appenines Moho, Alpine Moho and Ligurian Moho): depth estimation can be sometimes challenging. Recent seismicity studies proposed that a deeper subducting slab of Adriatic lithosphere could occur as well in this area and the question about the depth estimation resolution remains open.

Based on teleseismic dataset, we have used coherent depth phases detected on CTBTO arrays (comprehensive-test-ban treaty-organization), using cepstral methods as well as focal mechanism estimations from genetic algorithm inversions to constrain the depths of all recent events above magnitude 3.8 in this area. The use of the teleseismic records gives the opportunity to reduce uncertainties due to complex crustal propagations during regional depth estimations. Moreover, pmP reflexions, observable on some teleseismic records, prove that, at least one event, (January 27, 2012) occurred below the Moho discontinuity, strengthening the hypothesis of the active slab.

Then, we have focused on characterizing the link between depth and stress drop, as it is a crucial parameter for ground motion prediction models. Hence, In addition of our new improved depth catalog, good stress drops evaluations are needed. These stress drops have been extracted from source spectra (magnitudes and corner frequencies, assuming Brune 's model), using the regional North Italy dataset collected in the last years by the strong-motion network (RAIS, INGV). We have used an iterative Gauss-Newton method developed by Drouet et al. (2011), which aims to separate source, sites effects and propagation contributions in the acceleration spectra. Inverted attenuation parameters are similar to those estimated by Castro et al. (2013) and sites effects have been checked to be coherent with the H/V profiles from the RAIS web site (http://rais.mi.ingv.it/), which strongly validate the isolated source spectra, thus, the associated stress drops. Finally, depth and stress drop are shown to be strongly correlated as depth events show high stress drop. Hence, in the global aim to predict ground motions, it seems that depth should be taken account in a more systematic way; especially as new seismic equipments (for instance CTBTO arrays) afford now better resolution for this crucial parameter.

Keywords: depth, stress drop, teleseismic, Po Plain, parametric inversion, corner frequency

Japan Geoscience Union Meeting 2013
(May 19-24 2013 at Makuhari, Chiba, Japan)

SSS28-15 Room:303 Time:May 23 11:00-11:15

Relationship between fc and Mo for AE from continuous and broadband records under a triaxial compressive condition

Nana Yoshimitsu[1*], Hironori Kawakata[2], Naoki Takahashi[3]

[1]Earthquake Research Institute, the University of Tokyo, [2]Ritsumeikan University, [3]Sumitomo Mitsui Construction Co., Ltd.

Micro fractures observed in laboratory experiments (acoustic emission; AE) have been studied to investigate a detailed faulting process [e.g., Yanagidani et al., 1985; Lockner et al., 1991]. To apply findings obtained in laboratory to field scales, it should be revealed that whether source characteristics of micro fracture is common with natural earthquakes or not due to large differences in scale. Seismic moment and corner frequency are fundamental parameters that characterize the source properties of the earthquake rupture. Down to events having a moment magnitude about -4, seismic moment thought to be proportional to cube of corner frequency [e.g., Abercrombie, 1995; Kwiatek et al., 2011]. However, it is still unclear whether AE size events also satisfies this relationship.

Previously, PZT elements which have narrow frequency ranges were often used as AE sensors, but their record were unsuitable for source parameter estimation. To overcame this problem, Sellers et al. [2003] tried to record AE with broadband transducers under a uniaxial rock fracture experiment. Though they indicated that the source parameters of AE events satisfied the same scaling relationship as that of natural earthquakes, the scaling relationship of AE themselves was still unconfirmed. In this study, we achieved multi-channel, broadband and continuous recording of AE and estimated source parameters of them in a higher accuracy.

We mounted nine broadband transducers (sensitive range: 100 kHz - 2000 kHz) that were hermetically sealed with metallic cases around a cylindrical Westerly granite sample (100 mm in height and 50 mm in diameter). Sampling rate was 20 MS/s per channel. Loading was continued until differential stress decreased (46 MPa) after the peak strength (296 MPa), under a confining pressure of 10 MPa.

We focused on two clusters of events (around 1000 events) which occurred after the peak strength was reached. The hypocenters of each event in a cluster located less than 2 mm apart, and correlation coefficients exceeded 0.80 for four or more channels in the cluster. After the spectral correction, we obtained displacement spectra for S waves. We estimated corner frequency and seismic moment for events with sufficiently high signal-to-noise ratios.

Corner frequencies and seismic moments obtained from AE events in each cluster (moment magnitude of events are around -8 to -7) satisfied the scaling relationship that applies to natural earthquakes. In addition, they were found to satisfy the same scaling relationship for AE events alone. Stress drops of events were distributed from 0.4 MPa to 12 MPa.

This result indicates self-similar relationship between micro fractures in laboratory and natural earthquakes.

Keywords: corner frequency, seismic moment, scaling, AE, rock fracture experiment

SSS28-16 Room:303 Time:May 23 11:15-11:30

Microruptures concentrating on pre-existing planes at 1 km depth in a South African gold mine and their high b-values

Makoto Naoi[1*], Masao Nakatani[1], Kenshiro Otsuki[2], Yasuo Yabe[2], Thabang Kgarume[3], Gilbert Morema[4], Joachim Philipp[5], Sifiso Khambule[6], Thabang Masakale[6], Luiz Ribeiro[4], Hirokazu Moriya[2], Osamu Murakami[7], Shigeki Horiuchi[8], Hironori Kawakata[7], Nana Yoshimitsu[7], Koji Miyakawa[1], Atsushi Watanabe[1], Tony Ward[4], Ray Durrheim[3], Hiroshi Ogasawara[7]

[1]Univ. of Tokyo, [2]Tohoku Univ., [3]CSIR, [4]Seismogen, [5]GMuG, [6]OHMS, [7]Ritsumeikan Univ., [8]Home seismometer corp.

We deployed an Acoustic Emission (AE) sensor array, which can detect small ruptures down to Mw -5, at 1 km depth in the Cooke 4 shaft (previously known as Ezulwini mine) in South Africa, where up to Mw 3 class earthquakes are indued by mining of a planar gold reef. Naoi et al. [2012; SSJ fall meeting, poster] determined hypocenters by an automatic picking program [Horiuchi et al. 2011] and estimated Mw for 365,237 events. Ninety percent of those were located near mining fronts (hereinafter referred to as stope cluster), whereas most of the remainder belonged to planar clusters apart from the stope-cluster (hereinafter referred to as planar cluster). Naoi et al. [2012] investigated the stope-cluster AEs and showed that they obeyed the GR law with b = 1.3 from Mw -3.7 to 0. The b-value did not depend on time from blasting, even for 0-1min after blasts. Naoi et al. [2012] also confirmed the size distributions of earthquakes detected by mine's seismic network, which were dominated by stope-cluster events, obeyed the GR law with b = 1.3 from Mw -1.2 to 1 (To extract a sufficient number of events, catalogue for longer period and larger volume were used for the mine's seismic network). These suggest that stope-cluster events compose a population obeying the GR law with b = 1.3 between Mw -3.7 and 1.

The present study focus on planar-cluster AEs. We identified 7 planar clusters whose spatial extents were 10 - 80 m, which were located 20 - 70 m away from the mining front and were composed of 314 - 8667 AEs. Position and attitude of one of these clusters was consistent with a large geological fault (named Zebra fault) surrounding which our AE network was deployed. Also, corresponding weak planes (seemed to be joints) were found in tunnel for two other clusters. The remainders are thought to be related to unknown pre-existing weak planes that were not accessible for observation. Because event rates in these planar clusters were nearly constant during the analysis period and because no large earthquake occurred around them whose rupture extent could reach the extents of these clusters since 2009, when mining was started around the AE array, AEs of the planar clusters were judged to be steady activities, not aftershocks of large earthquakes. Relocated hypocenters of these planar clusters by Double Difference method [Waldhauser and Ellsworth, 2000] revealed that their distribution is so sharp that most hypocenters were aggregated within a thickness of 50 cm at the narrowest, sometimes event delineating stepovers and branches. These clusters were unrecognizable unless very small AEs were observed, because the 99.8% of the AEs in these planar clusters were smaller than Mw -2. Particularly, the maximum event in the planar cluster delineating Zebra fault was only Mw -3.0. The size distributions of the planar clusters followed the power law, and their slopes (b-value) were 1.38 to 2.19, which are higher than b-value of stope-cluster (b = 1.3).

Strong planar concentration of planar-cluster AEs observed in the present study is not necessarily consistent with microearthquake activities around active faults (e.g., Liu et al. 2003; Hauksson 2010). In addition, b-values of planar-cluster AEs were significantly different from typically observed b-values for natural earthquakes, whereas b-value of stope-cluster AEs was similar to those of natural earthquakes. This may be interpreted that size distribution of stope-cluster AEs and natural earthquakes reflect size distributions of weak planes in a volume region, whereas planar-cluster AEs are "microruptures" reflecting microscopic irregularities of a macroscopic weak plane (e.g., roughness of a fault); that is, planar-cluster AEs represent a different population from microearthquakes in the usual sense.

Keywords: Acoustic Emission, seismicity, South African deep gold mine

Japan Geoscience Union Meeting 2013
(May 19-24 2013 at Makuhari, Chiba, Japan)

SSS28-17 Room:303 Time:May 23 11:30-11:45

Energy Partition to Gouge Generation during Stick-slip as Studied by a New Large Biaxial Friction Ap

Tetsuhiro Togo[1*], Eiichi Fukuyama[2], Futoshi Yamashita[2], Kazuo Mizoguchi[3]

[1]Institute of Geology, China Earthquake Administration, [2]National Research Institute for Earth Science and Disaster Prevention, [3]Central Research Institute of Electric Power Industry

To determine how much of the frictional energy consume in generating fault gouge and breccia is important because this fraction will affect the energy used for frictional heating which in turn can affect the mechanical properties of a fault during seismic fault motion. In addition, it is geologically important to understand the formation and developing process of the mature fault zones.

We have used the large biaxial machine newly constructed in National Research Institute for Earth Science and Disaster Prevention (NIED), Tsukuba (Fukuyama et al. 2012 and Yamashita et al. 2012). This machine is developed to bridge a scale-gap between natural earthquakes (~km) and conventional laboratory experiments (~mm). The machine is built on the shaking table and used the hydraulic actuator of the table as the shear loading jack.

We have conducted seven biaxial friction experiments on Indian gabbro at average slip rates of 1.09 to 110 mm/sec, at normal stresses of 0.66 to 1.32 MPa and with displacements to around 0.42 m. Rectangular specimens of 1.5 $*$ 0.5 $*$ 0.5 m and 2.0 $*$ 0.5 $*$ 0.5 m with the surface irregularity less than 24 microns are used. The same specimens are repeatedly used in all experiments but the generated gouge was collected in each experiment by using the brush to measure the surface energy.

All experiments showed violent stick slip events except for the first run (v = 1.09 mm/s, normal stress = 0.67 MPa) where a stick-slip amplitude increased from small to moderate values with increasing displacement. Overshooting of shear stress occurred during some stick-slip events at slip rates of 10 mm/s and 100 mm/s; that is, shear stresses dropped down to negative values during some stick-slip events. The entire stiffness of the apparatus and shaking table was determined as $1.19*10^8$ N/m by using shear force drop (dF) and the displacement during slipping stage (dD) in each stick-slip event suggested by Shimamoto et al. (1980). This value is consistent with the quasi-static analysis.

The energy fraction of the gouge generation is determined by the surface energy of gouge divided by the frictional energy during each experiment (Togo and Shimamoto, 2012). Specific frictional energy in each experiment was obtained by the integration of the shear stress multiply displacement and the values were 0.18 to 5.16 MJ/m^2. Total surface energy of generated gouge in each experiment (E_A) was obtained the following equation.

$E_A = A_{BET} * r * m$

Where A_{BET} is the specific surface area of generated gouge, r is the surface free energy and m is the mass of the generated gouge. Specific surface area was measured by the BET surface area using a BELSORP-mini made by BEL Japan, Inc. with nitrogen as adsorbate. Specific surface area of the generated gouge showed high value of 5.29+-0.59 m^2/g at the first two experiments and it decreased with the increasing of the cumulative displacement to around 2.20+-0.49 m^2/g and total surface energy of generated gouge was 37.3 to 627.0 J. Results show that grain crushing absorbed only $9.63*10^{-4}$ to $1.39*10^{-1}$ % of frictional work. Thus, host rock wearing and gouge generation is unlikely to be an important energy sink at least for mature faults with well-developed slip zone.

Japan Geoscience Union Meeting 2013
(May 19-24 2013 at Makuhari, Chiba, Japan)

SSS28-18 Room:303 Time:May 23 11:45-12:00

Numerical analysis of failure of soil ground due to surface loading and generation of vibration induced by the failure

Akira Asaoka[1], Shotaro Yamada[2*], Toshihiro Noda[2]

[1]Association for the Development of Earthquake Prediction, [2]Nagoya University

In modern soil mechanics/geo-mechanics, the failure of soil ground has been analyzed as a progressive failure, in which elasto-plastic nature is introduced for the soil behavior. The main target of the analysis is the prediction of both the shape and the location of strain localization area in the ground and they intend to observe, through computation, how the strain localization area develops progressively with time and with space. The analysis is then somewhat different from the conventional slip failure analysis in which the shape and the location of failure zone and/or slip line are usually considered as given conditions for the analysis[1), 2)].

In this study, the so called "bearing capacity problem" in soil engineering is newly analyzed as an example problem of the progressive failure of soil ground, in which vibration behavior of the ground is first observed, through computation, during the whole procedure of progressive failure. The numerical analyses are performed using the soil-water coupled finite deformation analysis code ***GEOASIA***[3)] that mounts the SYS Cam-clay[4)] elasto-plastic soil model on it. In the analysis, since the rate type equation of motion is precisely time-integrated, then progressive failure will be completely analyzed as a nonlinear dynamic problem.

First considered was the case of "displacement control loading" in which loading to the ground is applied with constant rate of displacement of foundation. In this case, the soil ground exhibited localization of deformation and formation of a circular arc-shaped slip failure. At the same time "load reduction" was also observed with the development of failure zone. To the same soil ground, surface load was next applied by the "load control" method. In this case, after the applied load reached the peak load, the soil ground suddenly failed and dynamic motions with acceleration were observed at the foundation under the same amount of applied load. Very much irregular vibration was also observed in surrounding ground due to the "shock" of the failure[5)]. In the vibration, very high frequency components were found to dominate, the reason for which will be due to the small scale of foundation. Focused on this point, the analysis objects were next scaled up 300 times big (from 8m high and 96m wide to 2.4km high and 24.8km wide). In this case, the dominant period of the vibration acceleration in surrounding ground shifted from about 0.2-0.3 seconds to about 5-8 seconds, keeping the amount of maximum acceleration almost the same. The descent of shear stress in slip/failure region that led to both the "load reduction" and the dynamic motion of foundation will be delivered later.

Recently, geo-materials have been obtained from deep subduction zone of huge plates. Although the authors have not seen such geo-materials yet, they intend to make research works that describe the change of elasto-plastic properties of such geo-materials that should have occurred due to the subduction zone slip failure using the computational elasto-plastic geo-mechanics.

References:

1) Asaoka, A., Nakano, M. and Noda, T. (1994): Soil-water coupled behaviour of saturated clay near/at critical state, *Soils and Foundations*, **34(1)** , 91-106.

2) Noda, T., Yamada, S. and Asaoka, A. (2005): Elasto-plastic behavior of naturally deposited clay during/after sampling, *Soils and Foundations*, **45(1)**, 51-64.

3) Noda, T., Asaoka, A. and Nakano, M. (2008): Soil-water coupled finite deformation analysis based on a rate-type equation of motion incorporating the SYS Cam-clay model, *Soils and Foundations*, **48(6)**, 771-790.

4) Asaoka, A., Noda, T., Yamada, E., Kaneda, K. and Nakano, M. (2002): An elasto-plastic description of two distinct volume change mechanisms of soils, *Soils and Foundations*, **42(5)**, 47-57.

5) Noda, T., Xu, B. and Asaoka, A. Acceleration generation due to strain localization of saturated clay specimen based on dynamic soil-water coupled finite deformation analysis, *Soils and Foundations*, to be submitted.

Keywords: progressive failure, vibration, soil ground, elasto-plastic geo-mechanics, inertial force

SSS28-18 Room:303 Time:May 23 11:45-12:00

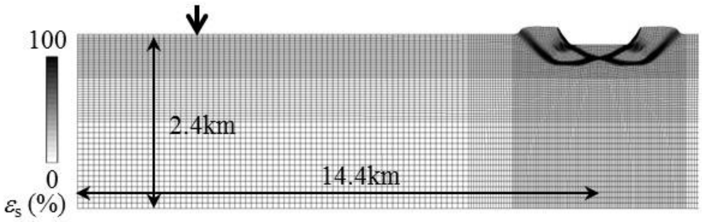

Fig. 1. Failure of ground with strain localization

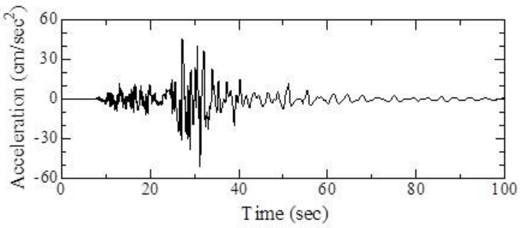

Fig. 2. Vibration in surrounding ground due to the shock of failure (at the point indicated by the arrow in Fig. 1.; vertical direction)

SSS28-P01 Room:Convention Hall Time:May 23 18:15-19:30

Fault plane heterogeneity determined by fractal geometry of fault zones

Kenshiro Otsuki[1*]

[1]Dept. Geol., Graduate School of Science, Tohoku Univ.

Investigation 1

Fault planes are inherently heterogeneous and this is a source of variety of earthquakes. Fault zones are composed of fault segments and jogs. Otsuki & Dilov (2005, JGR, 110, B03303) found for experimentally made fault zones of 1 mm order lengths that fault segments + jogs structures are hierarchically self-similar. With the additional data of small geological faults of a 10 m order length scale and strike-slip seismic faults longer than the thickness of seismogenic layer which emerged on the earth's surface, segment length $L_S(i)$, jog length $L_J(i)$ and jog width $W_J(i)$ show the correlations below,

$L_S(i+1) = 0.348\, L_S(i)^{0.994}$ approx. $L_S(i+1) = 0.365\, L_S(i)$ —— (1)

$W_J(i) = 0.0278\, L_S(i)^{1.06}$ approx. $W_J(i) = 0.0402\, L_S(i)$ —— (2)

$W_J(i) = 0.191\, L_J(i)^{0.990}$ approx. $W_J(i) = 0.189\, L_J(i)$ ——— (3),

where i denotes the hierarchical rank. These relations indicate the fractal dimension D of fault zone geometry is close to 2.

For the individual three data set eqs. (2) and (3) are represented by $W_J(i) = b\, L_S(i)^H$, $W_J(i) = a\, L_J(i)^A$ with different proportional constants and power values.

For experimental faults......... b=0.00385, H=0.642, a=0.00694, A=0.516.

For geologic small faults....... b=0.333, H=0.763, a=0.141, A=0.558.

For strike-slip surface faults.. b=0.164, H=0.853, a=3.18, A=0.665.

Investigation 2

Seismologists have searched for appropriate distribution patterns of the heterogeneity which can explain the G-R law and the k^{-2} falloffs of earthquake displacement spectra (e.g. Madariaga, 1979, JGR, 84, 2243; Andrews, 1980, JGR, 85, 3867; Frankel, 1991, JGR, 96, 6291; Herrero & Bernard, 1994, BSSA, 84, 1216). They reached the conclusion that D is 2 if static stress drop is constant. This is very consistent with the analytical results for fault zone geometry mentioned above. The parameter H corresponds with the Hurst exponent, and it is related with D by D=E+1-H, where E denotes Euclidean dimension. Since H=0.853 for strike-slip seismic surface faults, D=2.15. Mai & Beroza (2002, JGR, 107, B11,2308) analyzed the slip distributions which were depicted by waveform inversions for many earthquakes, and found that D=2.29 and H=0.75 at an average, being consistent with my results.

Investigation 3

Mai & Beroza (2002, JGR, 107, B11,2308) estimated for correlation distances of slip distributions on fault planes to be about 1/3 of the effective fault lengths. Bersenev (2001, JGR, 28, 35) found that earthquakes are associated with sub-events with about 1/3 length scale of the main phases. These are consistent with eq. (1). It depicts that one overall fault zone is divided into three first-order segments, and that the fractal of fault plane geometry is not continuous but discrete (hierarchical). This discreteness is supported by the numerical simulations by Ben-Zion & Rice (1995, JGR, 100, 12959) in which real complex slip patterns were realized especially when strong and abrupt heterogeneities (of jogs) were assumed.

Investigation 4

Scholz (1982, BSSA, 72, 1) proposed that mean strike-slips are proportional to fault lengths even if the fault is much longer than the thickness of seismogenic layer (L-model). This curious problem has been open to discussion. My analytical results show that mean strike-slips U_m of surface large faults are related with fault lengths L_0 by the power function as,

$U_m = 0.246 {L_0}^{0.46}$ ——— (4).

Note that the power value is less than 1. This is caused by jogs which pin the fault slip to make faults stiffer. Only ${L_0}^{0.46}$ is interpreted to work as an fault length effective for slips. Recent numerical simulation results for seismic slips on heterogeneous fault planes (e.g. Hillers & Wesnousky, 2008, BSSA, 98, 1085; Dieterich & Smith, 2009, PAGEOPH, 166, 1799) realize such phenomena.

The relation with fracture surface energy and the evolution of fault zone geometry will be discuss elsewhere.

Keywords: fault plane, geometry, fractal, heterogeneity

Japan Geoscience Union Meeting 2013
(May 19-24 2013 at Makuhari, Chiba, Japan)

SSS28-P02 Room:Convention Hall Time:May 23 18:15-19:30

Numerical simulations for interactions of dynamic rupture on fault step-over

Keisuke Kanano[1*], Shoichi Yoshioka[2]

[1]Dept. of Earth and Planetary Sci., Kobe Univ, [2]RCUSS, Kobe Univ

Fault system on the Earth's surface consists of some segments with various structures such as bending, branching, and stepping. A part of stepping faults overlaps each other in many cases. In this study, we investigate interaction of dynamic rupture between two or more parallel planar vertical strike slip faults, and rupture stop in an overlapped zone, by spontaneous fault rupture simulations.

We used staggerd-grid split-node method (Dalguer and Day , 2007). As for the friction law, we assumed slip-weakening relationship. The initial stress field is assumed to be uniform, and elastic modulus is homogeneous. Assuming the three-dimensional orthogonal coordinate system, x axis is taken parallel to a fault plane, y axis is perpendicular to the fault, and z axis is taken downward(Earth's surface is z= 0 km). A fault is located in spatial range of -15 km$<$x$<$15 km, y= 0 km, and 0 km$<$z$<$15 km.This fault is hereafter referred to as Fault 1.The initial rupture zone is set in the central part of Fault 1. The second fault, which is Fault 2, is located in spatial range of -15 km$<$x$<$35 km and 0 km$<$z$<$15 km, changing the distance between the two faults in the y direction. Left lateral-strike slip faults were assumed, and extensional step was considered.

As a result, dynamic rupture of Fault 2 was triggered at the point located at the edge of Fault 1 (near x= 15 km) in all cases. After rupture was triggered on Fault 2, the rupture spread on the fault plane. In the overlapped zone, however, rupture on Fault 2 stopped spontaneously. This can be interpreted that shear stress drop in the overlapped zone on Fault 2 took place due to slip on Fault 1, causing difficulty for shear stress to reach strength on Fault 2. Simulated results for changing distance between the two faults showed that the smaller the distance is, the easier rupture stops in the overlapped zone on Fault 2, whereas the longer the distance is, the more difficult rupture stops on Fault 2. This is because the smaller the distance between the two faults is, the more the effect of shear stress drop by slip of Fault 1 on causing rupture on Fault 2 is large in the overlapped zone, whereas the larger the distance between the two faults is, the smaller the effect is. However, if the distance between the two faults is larger than a certain value, rupture on Fault 2 itself was not triggered anymore.

Keywords: step-over, spontaneous rupture simulation, rupture stop, staggerd-grid split-node method

Japan Geoscience Union Meeting 2013
(May 19-24 2013 at Makuhari, Chiba, Japan)

SSS28-P03 Room:Convention Hall Time:May 23 18:15-19:30

Slip stabilization, a counterintuitive slip response to a sudden buildup of loading stress, predicted by a revised rate

Nobuki Kame[1*], Satoshi Fujita[1], Masao Nakatani[1], Tetsuya Kusakabe[1]

[1]Earthquake Res. Inst., Univ. of Tokyo

Motivated by the existing discrepancies between the model predictions of Dieterich (1994) and the observed aftershock seismicity, we re-examined aftershock triggering on faults obeying the recently revised RSF incorporated with a newly noticed stress-weakening effect (Nagata et al., 2012) that seems eventually free from contradictions with laboratory friction experiments. Time-to-instability analysis, which is necessary as a specific nucleation model to get on the original theoretical framework of Dieterich's aftershock modeling, was numerically conducted to derive the resultant aftershock sequences obeying the revised RSF. It was found that certain improvements towards common observations, in terms of raised seismicity and shortened delay before Omori decay. However, the improvements were far too small to resolve the huge quantitative gap in the characteristic stress (direct effect coefficient 'a' times 'normal stress') between laboratory values and what is inferred from observed aftershock sequences. On the other hand, through many numerical simulations of slip response to a stress step imposed at different timings in the seismic cycle, we noticed a counterintuitive behavior of the revised RSF. When a sufficiently large stress step is imposed at a timing somewhat before entering self-accelerating stage of the seismic cycle, the timing of earthquake can be delayed rather than advanced. In this case, the earthquake will occur after several oscillatory cycles resembling slow slip events, which might be usable as a marker for a fault at a certain stage in the seismic cycle. This behavior itself is a potentially important finding in earthquake mechanics and a laboratory confirmation of the counterintuitive response of a frictional fault to a stress step, which is an unintended prediction by the revised RSF, is desired in the near future.

Reference

Kame, N., Fujita, S., Nakatani, M. and Kusakabe, T., Effects of a revised rate- and state-dependent friction law on aftershock triggering model, Tectonophysics (2012), http://dx.doi.org/10.1016/j.tecto.2012.11.028

SSS28-P04 Room:Convention Hall Time:May 23 18:15-19:30

Dependence of earthquake stress drop on scaling of frictional parameters

Shingo Yoshida[1*], Naoyuki Kato[1]

[1]ERI, Univ. Tokyo

To understand dependence of stress drop on scaling of frictional parameters, we conducted numerical simulation of earthquake cycles on plate interface. We assume a circular asperity which obeys a rate- and state-dependent friction law. If the critical slip length L is proportional to the asperity radius r, and b-a is a constant, stress drop is independent of the ruptured area size R. On the other hand, if L is a constant independent of r, stress drop decreases with increasing R because earthquake occurs before large stress is accumulated compared with the former case. Numerical simulation shows the stress drop is proportional to R^[-0.43]. Such a phenomenon is not observed for natural earthquakes. Kato (2012) reported that stress drop is proportional to R^[-0.5] on the basis of 2-d simulation results and theory of fracture mechanics if fracture energy is independent of asperity size.

Keywords: stress drop, scaling, rate- and state-dependent friction law, asperity

Japan Geoscience Union Meeting 2013
(May 19-24 2013 at Makuhari, Chiba, Japan)

SSS28-P05 Room:Convention Hall Time:May 23 18:15-19:30

Complicated recurrence of slip events on a uniform circular asperity

Naoyuki Kato[1*]

[1]Earthquake Research Institute, University of Tokyo

Numerical simulation of repeated occurrence of slip events on a fault patch (asperity) is conducted to understand the mechanism of irregular sequence of slip events. The fault is uniformly shear loaded at a constant rate, and frictional stress acting on the fault is assumed to obey a rate- and state-dependent friction (RSF) law. A circular patch with velocity-weakening frictional property is embedded in a fault with velocity-strengthening frictional property elsewhere. A numerical simulation is conducted by varying the characteristic slip distance L of the RSF law. Slip behavior changes as L increases. When L is small, seismic slip events (earthquakes) repeatedly occur at a constant time interval. As L increases, recurrence of slip events becomes complex. Period doubled slip pattern, where seismic and aseismic slip events alternately occur, multiperiodic pattern, and aperiodic patterns occur. At the same time, slip tends to be aseismic with increasing L. The distributions of shear stress on the fault before the slip events are variable because of variations of the residual stress in the preceding slip event and aseismic sliding during an interseismic period. This variation in shear stress causes the complex sequence of slip events. Iteration maps of the recurrence intervals of slip events are examined by taking a plot of Ti versus Ti+1, where Ti denotes the time interval between the ith and (i+1)th slip events. Each iteration map for aperiodic sequence of slip events is expressed by a simple curve, suggesting that the occurrence time of the next event is predictable from the previous time interval and the slip event sequence exhibits deterministic chaos. To compare the simulation result of sequence of slip events on a velocity-weakening patch embedded in a velocity-strengthening region, a numerical simulation of slip on a velocity-weakening patch enclosed by unbreakable barrier. In this case, no complex recurrence of slip events is observed. When L is smaller than a critical value, seismic slip events repeatedly occur at a constant interval. On the other hand, stable sliding occurs when L is larger than the critical value. This result indicates that the complex slip behavior for a velocity-weakening patch embedded in a velocity-strengthening region comes from the interaction between the velocity-weakening and velocity-strengthening regions.

Keywords: earthquake cycle, asperity, chaos, simulation, friction

SSS28-P06 Room:Convention Hall Time:May 23 18:15-19:30

Earthquake forecasting system based on sequential data assimilation of the slip on the plate boundary

Takane Hori[1*], Shin'ichi Miyazaki[2], Mamoru Hyodo[1], Ryoko Nakata[1], Yoshiyuki Kaneda[1]

[1]Japan Agency for Marine-Earth Science and Technology, [2]Graduate School of Science, Kyoto Univerisy

We are constructing an earthquake forecasting system based on sequential data assimilation of the slip on the plate boundary. We use SIS, a kind of particle filter for the data assimilation. The forward calculation is done using earthquake generation cycle simulation. From the simulation results, we estimate crustal deformation that can be compared to the observation of GEONET on land and DONET on the seafloor. We demonstrate numerical test of this system using synthetic data of seafloor deformation before virtual Tonankai or Nankai earthquakes. We also use real data set of GEONET to compare the results of earthquake generation cycles.

Japan Geoscience Union Meeting 2013
(May 19-24 2013 at Makuhari, Chiba, Japan)

SSS28-P07 Room:Convention Hall Time:May 23 18:15-19:30

A hypothesis of a super subevent associated with the 2011 Mw9.0 Tohoku Earthquake

Ichiro Kawasaki[1*], Hiroshi Ishii[1], Yasuhiro Asai[1]

[1]Tono Research Institute of Earthquake Science

Kawasaki et al. (2012) proposed a rectangle fault model for the 2011 Mw9.0 Tohoku earthquake to match the synthetic waveforms by the exact solution in a half space of Okada (1980) to overall features of the GPS high sampling data of GEONET and continuos stress recording at TOS, Toki, Gifu prefecture, of TRIES. One of their conclusions was that rupture of maim fault started 40 s after the origin time of JMA. However, since their model did not elucidate transverse component of GPS displacements especially remarkable in the south Kanto district, we reanalyze the data.

Fig.1 shows records sections of the transverse component of GPS data (black) and synthetic waveforms (red) by the main fault of Kawasaki et al. (2012) in three directions of N90W, N125W and N145W. A horizontal axis is arrival time of S waves as reduced by the S wave velocity of 3.8 km/s. Fig.1 means that the remarkable pulse between broken lines at 70 s and 95 s of the pulse width of 25 s to 30 s and the amplitude of up to 70 cm was SH waves propagating at the S wave velocity. Fig.1 also suggests that corresponding source was within or close to the main rupture area.

Since a low angle thrusting dipping to the west does not radiate SH waves to the west and radiate only small amplitude SH waves to the south, the source of the SH waves is supposed to be a subevent having a separate fault plane in which strike slip component is dominant.

Since a node of the SH wave polarity lies in an N80W direction, a strike direction of the subevent should be around N60E or N150E. Starting from initial model of vertical left lateral strike slip fault above the plate boundary, we attempt trial and error approach to propose the following rectangle subfault model: strike direction N145E, dip angle 85, slip angle 85, origin time 20 s after the initiation of main fault, depth 40km, fault length 30 km, width 20 km, rupture propagation velocity of 3.0 km/s to the southwest and upward, rise time 15 s, dislocation 200 m and seismic moment 5.3x1021 Nm (Mw8.4). This subevent elucidates characteristic features of the SH waves at many GPS stations and the stress record at TOS. The SH phase is within wavetrains due to the main rupture and thus ambiguity of the fault parameters is large. However, for the pulse width of 25 s to 30 s and the large amplitude of up to 70 cm, we are sure that the dislocation was extraordinary large compared with a fault size. In this sense, we would like to call it a super subevent.

Fig.1 Record sections of the transverse component of the GPS high sampling data (black) obtained at the time of the 2011 Tohoku earthquake in three directions of N90W, N125W and N145W. Red traces are synthetic waveforms by a main fault model of Kawasaki et al. (2012) and the half space calculation of Okada (1980). A vertical axis is displacement in meter. Vertical spacing is arbitrary. A horizontal axis is a travel time reduced by S wave velocity of 3.8 km/s, assuming the JMA origin time and epicenter.

Keywords: 2011 Tohoku earthquake, subevent, GPS high sampling data, Continuous stress records, dislocation velocity

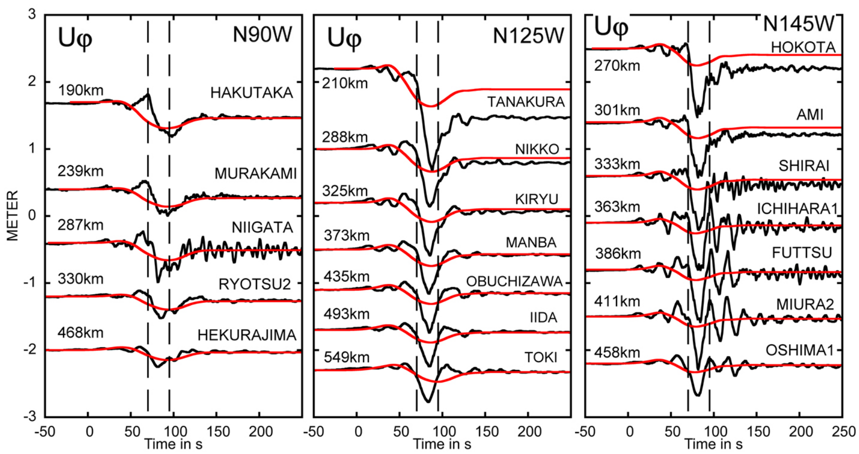

Japan Geoscience Union Meeting 2013
(May 19-24 2013 at Makuhari, Chiba, Japan)

SSS28-P08 Room:Convention Hall Time:May 23 18:15-19:30

Earthquake Energy Generation of Mw9 East Japan Off 2011

Shozaburo Nagumo[1*]

[1]Earthquake Research Institute, University of Tokyo

1. Purpose of the article

What on earth happened there, the Mw9.0 huge earthquake of East Japan off 2011. We present here a view. Firstly, the huge energy generation of Mw9 was done by the volume source, not by the plane source. Secondly, the huge energy-generation of Mw9 is a large-scale stress-adjustment activity, not the asperity rupture. The reasons are based on such observational facts as listed below.

2. Indicative features of volume source

(2-1) 3 big seismic-wave radiations. (2-2) The long duration time of seismic wave radiation. (2-3) The huge source area. (200km x 500km). (2-4) The oceanic mantle seismic activation (OBS observation)

3. Mechanism of volume source generation

Why it is a volume source? The theory of elasticity says that the seismic wave generation is the body force generation and the elastic strain-energy release. The earthquake source volume is the 3D region in which seismic waves are generated. Therefore body forces generate seismic waves. And the body forces are generated by vanishing elastic strain inside. One cause is due to the sudden crash of pores-and-cracks, and the other is due to the sudden change of the confining pressure. This is the generation of earthquake as well as volume source.

Because the geological rock body is regarded as a porous-cracked elastic body, and it is under the initial stresses of gravity and tectonic stresses. And the incremental stresses accumulate around the pores-and-cracks in long years..

4. Mechanism of the large-scale volume source generation

Why such a large-scale volume source is generated? The potential is the tectonic forces of the island-arc oceanic-trench system itself. Firstly, under the inclined surface, horizontal forces are generated towards the trench axis caused by the gradient of the self-weight pressure. Secondly, in the neighborhood of the trench, some upward and downward forces may be generated, probably metamorphism origin such as surpentinization and eclogite. Moreover, in the arc-side of the trench, the island-arc rock masses overload the underlying oceanic mantle. Thus, such forces generate a large-scale flexure and buckling deformations of the oceanic lithosphere. The buckling deformation leads to the elastic instability (Biot, 1965, Incremental Deformations). The scale of the instability is very large, more than several hundred km horizontally, more than 50km in depth including the overlying crust.

Its associated stress-distribution in such a broad region is block-wisely heterogeneous because of the tectonic history. Around the block boundaries, stresses concentrate and accumulate in long years. Thus the stress imbalance could exist broadly in the lithosphere of the island-arc and oceanic-trench system. Once the buckling fractures occur somewhere, these stresses could be successively released. This is the generation of the large earthquake and the large-scale volume source.

5. Process of stress-adjustment activity

How the huge area (200km x 500km) turned to the source area? At the beginning, a certain buckling fracture took place in the oceanic lithosphere, where the degree of deformations is high. The buckling fracture extended into the earth's crust leading to the detachment of rock-blocks. Then, the block-wise detachment released the confining pressure, and the rock masses were subjected to collapse, fracture and crash. These processes could correspond to the first 2 big seismic wave radiations in the northern part.

During these processes, the rock bodies loose its rigidity and are led to the fluidization, and caused the rock-flows. Such rock-flows are the shape deformation so as to decreases the gravity potential. The outward spreading rock-flow causes forces at the front as well as side-wards. Such a force might lead to the 3^{rd} big seismic wave radiation in the southern part. Such processes as above are the large-scale stress-adjustment activity to level the stress imbalance in a broad region. These processes are not the asperity rupture.

Japan Geoscience Union Meeting 2013
(May 19-24 2013 at Makuhari, Chiba, Japan)

SSS28-P09 Room:Convention Hall Time:May 23 18:15-19:30

Model that harmonizes with the rupture process of (Ide et al.2011)–Relation between 3.11 and off-Miyagi-earthquakes–

Hirofumi Mase[1*]

[1]none

I presented the model concerning the cutting plane that expresses the range from the coast to Japan Trench off Miyagi and passes the epicenter of the 3.11 Tohoku-Oki Earthquake. I formed with clay the wedge to a above plate, the subducting plate and the one located below it to a lower. I did the experiment pushing from right and left by the same power after they had been overlapped. The slip of the plate boundary started in the depth, and the Front of Slip rose aiming at the shallow. Afterwards, "Slip all together" of the entire boundary was generated because the shallow tip peeled off at a dash suddenly. I thought that the model had reproduced the feature off Miyagi and the process to 3.11 in 1,000 years.(above(1)) I also analyzed 42 remarkable past earthquakes in and around (2). I value (3) for the slip distribution and the rupture process of 3.11. I expect that the model will harmonize with (3) and past observation facts.

I clarified A) B) by the experiment afterwards. A)"Slip all together" is that the slip starts from "Hypocenter" and spreads to both the depth and the shallow. B)The deepest portion of the above plate started crushing the slope of the lower rather than slipping up. I placed a released paper between the plate boundary. Bigness and smallness in that effect influenced the passage of time to "Slip all together" and the overall amount of slip when ending. The event stagnates or ends imperfectly if the lower plate doesn't subduct smoothly beneath the above plate in the depth.

I was able to read C) from (3). I set straight line L of 50km or more in length that Onagawa-cho is made a starting point and expands to the south almost and reaches north latitude 38th parallel. C)In the change chart of time of slip velocity(40,60,75sec), the north and the south are excluded, the spread was dammed up once by the line L, and slip seems to have happened in the deepest portion at a dash afterwards(90sec) (3).

A) is the maximum result expected and it harmonizes with (3). B) and C) harmonize. Therefore, it can be said, the straight line that passes the middle point of the line L and the epicenter of 3.11 is "Center axis" of the compression system off Miyagi.

Though I explained the mechanics of the Earthquakes off Miyagi(EOFM), I interpreted for them to have happened usually because the Standoff before "Slip all together" had continued long in (1)experiment (2). However, there is the following facts. (a)The Standoff was able to be shortened easily B). (b)Slip in the depth that came off from the hypocenters of EOFM after 1936 was large (3). (c)[1936M7.4][1937M7.1][1978M7.4][2005M7.2][2005M6.6][2010M5.5] approach the epicenter of 3.11 almost in order of generation along "Center axis" (4)(2).

The row of hypocenters of (c) is not corresponding to the plate interface (2), and the distance has been still left for the hypocenter of 3.11 in addition. However, because a main shock extends within the considerable range and many aftershocks are accompanied usually, they(c) have the possibility of peeling off the boundary forward much and, needless to say, destroying the vicinity of theirself-hypocenter. Aren't EOFM synonymous with the progress of the Front of Slip ?

(1)[Mase]http://jglobal.jst.go.jp/public/20090422/201202271822634851
(2)[Mase]http://homepage3.nifty.com/hmase/upload120927web.htm
(3)[Ide]http://www.s.u-tokyo.ac.jp/ja/press/2011/12.html
(4)[JMA]http://www.seisvol.kishou.go.jp/eq/gaikyo/monthly

Japan Geoscience Union Meeting 2013
(May 19-24 2013 at Makuhari, Chiba, Japan)

SSS28-P10 Room:Convention Hall Time:May 23 18:15-19:30

Development of Complex Seismic Source Inversion Method: Application to December 7, 2012 Sanriku-oki Earthquake

Amato Kasahara[1*], Yuji Yagi[1]

[1]Life and Env. Sci., Univ. of Tsukuba

Good knowledge of the seismic source process is important for understanding the stress regime and physical properties in and around the seismic source area. However, it is difficult to directly observe the co-seismic behavior on a fault in the interior of the Earth. Hence, many seismic source inversion methods have been developed, since the pioneering study of Trifunac (1974), to estimate the seismic source process using geophysical observations available on the earth's surface, under the assumption that the seismic energy was released by a hypothetical fault plane. Usually a simple planar fault is assumed and its geometry is decided from one of the nodal planes of the corresponding Centroid Moment Tensor (CMT) solution. However, it is well known that surface traces of faults are bending and branching; moreover, the complexity in fault geometry is also supported by the existence of earthquakes whose focal mechanism solution, determined using P-wave first-motion polarities, is different from their CMT solution and events for which the CMT solution contains large Compensated Linear Vector Dipole components.

Inversion with inappropriate fault geometry could result in a biased solution and increase the risk of misinterpretation. To mitigate the problem, it is better to estimate not only the seismic source process but also the fault geometry at the same time.

We developed a seismic source inversion method that does not require prior information of detailed fault geometry. In this approach, the seismic rupture process is formulated as a moment release function in a volume around the seismic source and the fault location is represented as a region of high moment release density within the rock volume.

First, we performed a synthetic test for the new method. In the test, both mechanism solution distribution and moment release were well recovered through the method. Next, we applied the method to real data from an earthquake occurred on Dec 7, 2012 at Far East of Honshu, Japan. We found that both a thrust type and a normal type earthquake occurred closely in space and time. The earthquake ruptured mainly two patches, one was a reverse faulting patch in deeper part, east of the hypocenter, the other was a normal faulting patch in the shallow part, west of the hypocenter. The normal faulting patch extended down to about 40 km, which is consistent with the deepest normal faulting events observed after the 2011 Tohoku earthquake in the region (Obana et al., 2012). The hypocenter was located between the reverse faulting patch and the normal faulting patch, where the stress state seems to be approximately neutral. The rupture seems to have propagated bidirectionally from the hypocenter towards both the reverse and normal faulting regions.

Keywords: source process, inversion, December 7, 2012 Sanriku-oki earthquake

Japan Geoscience Union Meeting 2013
(May 19-24 2013 at Makuhari, Chiba, Japan)

SSS28-P11 Room:Convention Hall Time:May 23 18:15-19:30

Source mechanism of the eastern Mino earthquake (Mj 5.1) with Isochron Backprojection Method

Makoto OKUBO[1*], Atsushi Saiga[1]

[1]TRIES, ADEP

An earthquake (eastern mino earthquake; Mj 5.1) has occurred beneath the high density seismogram networks (HDSN; cf. Aoki *et al.* 1999 and Okubo, 2011) that consisted with more than 50 stations among 30km x 20km area on the 14th Dec. 2011. This earthquake had normal faulting type mechanism in subducting philipine sea slub (Saiga and Okubo, reviewing). Seismic motion of this earthquake includes high frequency components (Okubo and Saiga, 2012; JPGU), we can resolve detailed rupture process using with the dense seismogram networks and the high frequency phenomena.

In order to analyze rupture process of the eastern mino earthquake, we applied isochron backprojection method (IBM; eg. Festa and Zollo, 2006, Pulido *et al.*, 2008). We used the waveform records of our stations and some Hi-net (Obara *et al.*, 2002) observatories within 65 km hypocentral distances as datasets of IBM. First, we picked up S wave arrival time from waveforms, and calculated acceleration amplitudes. And we estimated the S wave velocity structure around the epicenter from Matsubara *et al.*(2008) with Vp/Vs = 1.73 assumption. And also we assume that rupture velosity does not beyond the S wave velocity and the maximum rupture length does not extend above the Matsuda's fault length-Magnitude relation (Matsuda, 1975), in IBM analysis.

We will discuss rupture process of the eastern mino earthquake and relations with aftershock hypocenters distribution, in presentation.

Keywords: source mechanism, main rupture, s waveform, dense seimometer array, high frequency seismic motion

Japan Geoscience Union Meeting 2013
(May 19-24 2013 at Makuhari, Chiba, Japan)

SSS28-P12 Room:Convention Hall Time:May 23 18:15-19:30

A deep revers outer-rise earthquake triggered a shallow normal outer-rise earthquake - The 2012 Off-Sanriku earthquake -

Tomoya Harada[1*], Satoko Murotani[1], Kenji Satake[1]

[1]Earthquake Research Institute, the University of Tokyo

The Dec. 7, 2012 Off-Sanriku outer-rise earthquake (Mj7.4) had two successive sub-events, the first sub-event was a deep reverse event (Event 1) and the second one was a shallow normal event (Event 2), as revealed by the teleseismic body-wave analysis (Kikuchi and Kanamori, 2003). The estimated coseismic slip distributions show that Event 1 had a relatively simple circular slip distribution and Event 2 had two large slips. Calculated static changes in the Coulomb Failure Function (dCFF) due to Event 1 shows positive values around the Event 2' s rupture area, indicating that Event 2 was induced by Event 1.

After the 2011 Tohoku earthquake of M 9.0, many outer-rise earthquakes have occurred near the Japan Trench and the Dec. 7, 2012 Off-Sanriku (Mj 7.4) was one of such outer-rise events. In this study, we estimated mechanism solution for this event by using the Kikuchi and Knanamori (2003)'s teleseismic body-wave analysis programs. We used UD-component of P-waveforms recorded at 73 stations with distance from 30 to 90 degree and assumed two triangles as source time functions. The result shows that the 2012 Off-Sanriku earthquake had two successive sub-events, the first event was a deep reverse event (Event 1; depth: 56 km, strike: 171.8 deg., dip: 57.3 deg., rake: 68.5 deg.) and the second event was a shallow normal event and it took place 20 sec. later at 20 km from Event 1 in the N25deg.E direction (Event 2; depth: 6 km, strike: 23.7 deg., dip: 76.3 deg., rake: -94.5 deg.). Seismic moments of Event 1 and 2 are 5.9*10^19 Nm (Mw7.1) and 7.8*10^19 Nm (Mw7.2), respectively, and 8.8*10^19 Nm (Mw7.2) in total. According to the Quick CMT Catalog, the reverse earthquake of Mw7.2 occurred at 144.09 deg. E, 38.01deg. N, and 58 km in depth, and normal earthquake of Mw7.2 followed 12 sec. after at 143.83 deg. E, 37.77 deg. N and 20 km in depth.

We then estimated coseismic slip distributions of Event 1 and 2 by the teleseismic body-wave inversion. The mechanism solutions and the point source locations estimated in the previous analysis were used for the initial mechanism and the rupture points, respectively, of both events. The coseismic slip of Event 1 is concentrated around the initial rupture point, with the maximum slip and average slip of 2.52 m and 0.43 m, respectively. As for Event 2, we used the residual waveforms that the synthetic waveforms from the slip distribution of Event 1 are subtracted from the observed waveforms. The slip distribution has two large slips. The maximum slip and average slip are 2.35 m and 0.82 m, respectively.

Finally, we calculated the static changes in the Coulomb Failure Function (dCFF) due to Event 1's slip distribution on steep nodal plane by using the Okada (1992)'s program. The positive dCFF is distributed in the shallow part of outer-rise region including the rupture area of Event 2. Therefore, we conclude that Event 2 was triggered by Event 1.

Keywords: outer-rise earthquake, tele-seismic body-wave analysis, coseismic slip distribution, dCFF

Japan Geoscience Union Meeting 2013
(May 19-24 2013 at Makuhari, Chiba, Japan)

SSS28-P13 Room:Convention Hall Time:May 23 18:15-19:30

Rupture Process of Moderate-Size Earthquakes by the MeSO-net

Ko Nishizawa[1], Takumi Murakoshi[1*], Yasuyuki Iwase[1], Takao Eguchi[1], Shin'ichi Sakai[1], Shigeki Nakagawa[2], Naoshi Hirata[2], Ryou Honda[3], Hisanori Kimura[4]

[1]National Defense Academy, [2]ERI, Univ. of Tokyo, [3]Hot Springs Research Institute of Kanagawa Prefecture, [4]NIED

The purpose of this study is to obtain the rupture process of moderate-size earthquakes in space and time by using waveforms in the Metropolitan Seismic Observation Network (MeSO-net). The MeSO-net is high-density seismograph network in and around the Tokyo metropolitan area, Japan. About 300 seismic stations are installed in the average intervals of several kilometers.The average station-to-station distance in MeSO-net is less than a quarter of existing seismic networks in Japan, where the average distances in K-net and KiK-net are about 20 km. In this study, we analyzed the fault motion of moderate-size earthquakes in and around Kanto region, Japan by applying the back-projection method to seismic waveforms in MeSO-net. We obtained detail images of the rupture process of moderate-size earthquakes.

Keywords: back-projection method, rupture process, MeSO-net, moderate-size earthquake

Japan Geoscience Union Meeting 2013
(May 19-24 2013 at Makuhari, Chiba, Japan)

SSS28-P14 Room:Convention Hall Time:May 23 18:15-19:30

Estimation of Radiated Seismic Energy from Regional and Teleseismic Waveforms

Ryota Kiuchi[1*], MORI, James[1]

[1]DPRI, Kyoto University

Therefore, it is important to compare different methods for estimating the radiated energy. Especially, we are interested in studying the apparent stress (rigidity multiplied by the ratio between radiated energy and seismic moment) of strike-slip earthquakes in the oceanic lithosphere, because it is often high (Choy and McGarr, 2002). However, this result is obtained from teleseismic P waves, and it is often difficult to correct for the radiation pattern of nodal arrivals, therefore, the estimated apparent stress may have a large variations.

In this study, we estimated the radiated energy for two large strike-slip earthquakes in Japan, the 2000 western Tottori earthquake (Mw 6.7) and the 2005 West off Fukuoka Prefecture earthquake (Mw 6.6), using both regional (less than 100km) and teleseismic (30deg < delta < 90deg) waveforms. To estimate the energy correctly, it is necessary to account for source effects (e.g.,radiation pattern) and path effects (e.g.,attenuation). We use only P waves for the teleseismic waveform, because of the strong attenuaion of teleseismic S waves and interference with other phases. For the teleseismic waveforms we need to account not only direct P but also depth phase, pP and sP (Boatwright and Choy, 1986).

The results show that the radiated energy of two earthquakes are not high. We will examine the each data carefully, and evaluate the differences in results from the different teleseismic and locally recorded data.

Keywords: radiated energy, apparent stress, strike-slip earthquake

SSS28-P15 Room:Convention Hall Time:May 23 18:15-19:30

Aftershocks Properties of the 2010 ML 6.4 Jiashian earthquake in Southern Taiwan

Chi-Chia Tang[1*], Cheng-Horng Lin[1]

[1]Institute of Earth Sciences, Academia Sinica

Large earthquakes often occur in unexpected locations and are followed by numerous aftershocks. Nevertheless, the aftershock properties of large earthquakes are not usually discovered in detail because a significant portion of aftershock sequences is missing in existing earthquake catalogues, mainly due to overlapping arrivals of seismic waves from these events. We examined waveform data of aftershocks of the 2010 ML 6.4 Jiashian earthquake recorded by the 19 stations of the Central Weather Bureau Seismic Network. We utilize a matched filter technique which Peng and Zhao (2009) used in detecting early aftershocks to discovery missing aftershocks. We use waveforms of 574 aftershocks as templates and scanned three-day data since the original time of mainshock. We identify ~ 4 times more aftershocks than listed in the catalogue of Central Weather Bureau. We find that newly detected events mainly concentrated within first 24 hours and most of them occurred with magnitudes < 2.0. The aftershocks migrated westward from the epicenter of mainshock, ~ 90 degree counterclockwise from the trend of adjacent faults. The seismicity rate of detected aftershocks is proportional to the inverse of time since the mainshock following the Omori Law.

Keywords: Aftershock, Jiashian, Taiwan

Japan Geoscience Union Meeting 2013
(May 19-24 2013 at Makuhari, Chiba, Japan)

SSS28-P16 Room:Convention Hall Time:May 23 18:15-19:30

An Adjoint Data Assimilation Method for Optimizing Frictional Parameters on the Afterslip Area

Masayuki Kano[1*], Shin'ichi Miyazaki[1], Kosuke Ito[2], Kazuro Hirahara[1]

[1]Kyoto Univ., [2]JAMSTEC

Afterslip sometimes triggers another earthquake in the time-scale of days to several years. Thus it may be possible to predict the occurrence of such a triggered earthquake by simulating the spatio-temporal evolution of afterslip with the estimated frictional parameters. To demonstrate the feasibility of this idea, we consider a plate interface model where afterslip propagates between two asperities following a rate and state friction law and adopt an adjoint data assimilation method to optimize frictional parameters. Synthetic observation data are sampled as the slip velocities on the plate interface during 20 days. It is found that 1) all frictional parameters are optimized if data set consist not only of the early phase of afterslip or acceleration, but also of decaying phase or deceleration and 2) that the prediction of the timing of the triggered earthquake is improved by using adjusted frictional parameters.

Keywords: afterslip, frictional parameters, data assimilation

Japan Geoscience Union Meeting 2013
(May 19-24 2013 at Makuhari, Chiba, Japan)

SSS28-P17 Room:Convention Hall Time:May 23 18:15-19:30

Source Parameter Study of Hydraulic Fracturing induced Microearthquakes using Empirical Green's functions

Ahyi KIM[1*], IIDA, Shuhei[1], RUTLEDGE, James[2]

[1]Yokohama City University, [2]Schlumberger

Hydraulic fracturing is a technique used to allow economic production of gas and oil from low-permeability reservoirs. The technique is also used to enhance geothermal energy development. Currently, microseismicity induced by the fluid injection is routinely monitored to map the fracture growth process in real-time. A natural development is to characterize the mechanism of the microearthquakes. Understanding source characteristics of these events is expected to provide a better understanding of the fracturing process and the influence of pre-existing structures controlling the distribution of events. Although several focal mechanism studies have been done in gas and geothermal field, its estimation is often biased due to various errors. Often the most significant difficulty in retrieving the source parameters in these monitoring studies is from poor azimuthal coverage. To avoid these uncertainties in this study, we estimate the source parameters using the empirical Green's function (eGf) analysis. The eGf approach is advantageous because it can be performed with one receiver, and requires no assumption of geologic model. We deconvolve the smaller event from the larger events recorded at the same receiver to obtain the source time functions of the larger events. We use the source-time functions to fit the seismic moment and corner frequency of the source-time spectra using a least-squares curve fit to the f2 spectra. The data we use were recorded during a hydraulic fracture imaging test in the Carthage Cotton Valley gas field of east Texas using two multi-level, three-component geophone arrays deployed in nearby monitoring wells. The treatments monitored include gel-proppant treatments using high viscosity fluids and low-viscosity water frac treatments In this study we apply the eGf method to the events precisely relocated from two injection stages ($-2.4 < Mw < -0.6$). Preliminary result indicates source spectra of most events agree well with double couple event. We also examine the correlation of the corner frequency and seismic moment to investigate whether those events follows the self-similarity observed in tectonic events.

Keywords: Hydraulic fracturing, Microearthquakes, Empirical Green's function, Source spectra, Source characteristics, Scaling Law

Japan Geoscience Union Meeting 2013
(May 19-24 2013 at Makuhari, Chiba, Japan)

SSS28-P18 Room:Convention Hall Time:May 23 18:15-19:30

AE in rock under triaxial compression with small perturbation of confining pressure - Comparison with b-value variation-

Takashi Satoh[1*], Xinglin Lei[1]

[1]GSJ/AIST

It is well known that seismic activity may be affected by small perturbation of crustal stress such as earth tide. Tanaka (2010, 2012) showed that the correlation between tidal stress and earthquake occurrence time had became significant since about 10 years before the 2004 Sumatra earthquake (Mw9.0) and 2011 Tohoku-oki earthquakes (Mw9.1), and it disappeared after the main shocks. The correlation was the highest around the hypocenter regions of these earthquakes. Nanjo et al. (2012) found similar space-time variation patterns of the b-value in Gutenberg-Richer frequency magnitude relation before and after these earthquakes.

In order to study effects of small stress perturbation on seismic activity, we have measured acoustic emissions (AEs) during triaxial compression experiments with small periodic perturbation of confining pressure (Pc). We reported so far experiments using granite samples drilled near the Nojima fault (Satoh & Lei, 2010), and that using a Westerly granite sample having artificial defects (Satoh & Lei, 2012). In this report, motivated by Nanjo et al. (2012), we compared the changes in the correlation between AE activity and Pc perturbation observed in these experiments with the b-value variation. It seems that the higher correlation between AE activity and Pc perturbation corresponds to the lower b-value, which is consistent with what observed for the M9 class earthquakes reported by Tanaka (2010, 2012) and Nanjo et al. (2012).

<References>

Nanjo et al., 2012, GRL, vol.39, L20304, doi:10.1029/2012GL052997.
Satoh & Lei, 2010, Seism. Soc. Japan, 2010 Fall Meeting, C11-04.
Satoh & Lei, 2012, Seism. Soc. Japan, 2012 Fall Meeting, D31-3.
Tanaka, 2010, GRL, vol.37, L02301, doi:10.1029/2009GL041581.
Tanaka, 2012, GRL, vol.39, L00G26, doi:10.1029/2012GL051179.

Keywords: Small periodic stress perturbation, AE activity, b-value

Japan Geoscience Union Meeting 2013
(May 19-24 2013 at Makuhari, Chiba, Japan)

SSS28-P19 Room:Convention Hall Time:May 23 18:15-19:30

A detailed view of the injection-induced seismicity in a carbonate gas reservoir in Southwestern Sichuan Basin, China

Xinglin Lei[1*], Shengli Ma[2], Wenkang[3], Chunmei Pang[3], Jie Zeng[3], Bing Jiang[3]

[1]Geological Survey of Japan, AIST, Japan, [2]Institute of Geology, China Earthquake Administration, [3]Zigong Earthquake Administration

Seismicity at a gas reservoir located in the relatively stable Sichuan Basin, China, mirrors the injection pressure of unwanted water, suggesting that the seismicity is injection induced. Injection under high pressure on a routine basis began on 9 Jan. 2009, and continued to July 2011. During the injection period, over 120,000 m^3 of water was pumped under a wellhead pressure of up to 6.2 MPa into the limestone formation of Permian 2.45 to 2.55 km beneath the surface. The injection induced more than 7,000 surface recorded earthquakes, including 2 M4+ (the largest one was ML4.4), 20 M3+, and more than 100 M2+ events. Data observed by a nearby local seismic network and five temporal stations provide a detailed view of the spatio-temporal distribution of the induced earthquakes. Most events were limited to depths ranging from 2.5 to 3.5 km, which is consistent with the limestone formation of Permian. In a map view, hypocenters are concentrated in a NNW extended ellipsoidal zone approximately 6 km long and approximately 2 km wide centered approximately 1 km northwest of the injection well.

The spatio-temporal distribution and other statistical results indicate that the triggered seismicity is characterized by four typical phases, which reflect the patterns of the injection rate and wellhead pressure. The largest ML4.4 events occurred when the wellhead pressure reached 0.9 MPa at the very beginning of injection. Various factors, such as the shear mechanism, the pattern of hypocenter distribution, and the fractal dimensions, indicate that the induced seismicity in the region resulted from the reactivation of pre-existing faults. Injected fluids diffuse outward along pre-existing faults, which were originally stressed, weakening the faults and leading to their reactivation. The intersections of a set of conjugate fractures are particularly suitable for fluid flowing. Some relatively large dipped faults likely bound the outward fluid flow and provide paths for upward leakage and downward flow.

The overall migration front follows a typical pore-pressure diffusion curve with a hydraulic diffusivity of 0.1 m^2/s. There are also some fast responses of seismicity on pressure change reflecting pore-pressure diffusion along the surface of pre-existing faults with a hydraulic diffusivity on the order of 1 to 10 m^2/s. Multi sources of evidence, such as the shear mechanism, pattern of hypocenter distribution, and small elevated pore pressure as compared with the least principal stress in the region show that the induced earthquakes occurred as a result of lowering of the effective normal stress on known or unknown pre-existing blind faults.

Keywords: Injection-induced seismicity, Gas field, Carbonate Reservoir, ETAS model, Pore-pressure

SSS28-P20 Room:Convention Hall Time:May 23 18:15-19:30

In-situ stress measurement at the closest proximity of an M1.5 earthquake at Tau Tona gold mine in South Africa

Hiroshi Ogasawara[1*], Gerhard Hofmann[2], Harumi Kato[3], Chris Stander[2], Gilbert Morema[4], Trevor Clements[5], Phil Piper[5]

[1]College of Science and Engineering, Ritsumeikan University, [2]Anglogold Ashanti Ltd. Rock Engineering, [3]Akema Boring Ltd., [4]Seismogen CC, [5]Ground Work Ltd.

In-situ stress measurements were successfully carried out in close proximity to a M1.5 damaging seismic event at 104 level (about 2950 m depth) at Tau Tona gold mine in South Africa. This event occurred on 3 December 2012, and on the 6th and 7th of February 2013, three overcoring stress measurements were done. The seismic event took place almost at the end of a pilot tunnel (see a photo attached), and significant dynamic rock mass ejection from the sidewall of the tunnel occurred. Elastic numerical modelling did not indicate any anomalous stress levels, but due to the severity of the damage it was important to better understand prevailing stress conditions. Stress measurement methods commonly used in South Africa (e.g. CSIR triaxial cell method or CSIRO HI method) was not suitable for such high stress conditions or adverse drilling conditions.

We used the BX CCBO technique (60mm diameter CCBO overcoring), a downsized version of the Compact Conic Borehole-end Overcoring technique (76mm diameter overcoring; Sakaguchi et al. 1992; Sugawara and Obara 1999; ISRM suggested). For overcoring, 6-15m BX pilot holes are drilled from tunnels at depths. Tools are used allowing implementation of the technique for typical South African geological drilling setups with small pneumatic machines. The procedure was first proven effective in South African gold mine conditions in 2011, on 98 L at Moab Khotsong Mine (about 3.0km depth) at an area with supposed minimal mining perturbation (Ogasawara et al. J. SAIMM 2012) . The technique was also implemented on 28 and 29th of January 2013 at Mponeng Gold Mine, 120L (an about 3350 m depth) also at an area with least mining stress perturbation.

At both the 3.0km-deep site at Moab Khotsong mine and the 3.4km-deep site at Mponeng mine, the measured maximum principal stress was consistent with overburden pressure. The determined orientations of intermediate principal stress (the horizontal maximum principal stress) and its ratio to the maximum principal stress was also consistent with the stress fields that well accounted for the fault slip mechanisms of nearby M2-4 earthquakes in the mines (e.g. Hofmann and Murphy 2007; Hofmann and Scheepers 2010).

At the moment, we have to wait for lab test for elastic modulus of the cores recovered from the measurement hole. However, if we used a typical elastic modulus for the lithology of the site, the measured stress at 104L (about 3.0km depth with least mining) at Tau Tona was much larger than the measured stress at 120L (a 3.4km depth with least mining) at Mponeng mine.

No in-situ stress measurements have been carried out close to the area of the damaging seismic event before, and hence no stress information was available towards mitigating seismic risk. It was proven that the BX CCBO technique can be implemented in adverse underground conditions - high stress and limited shift working hours in the South African gold mines. We hope that stress measurement can be done regularly together with a pilot geological drilling program, prior to advancing the pilot tunnel, which will fundamentally contribute to mitigate seismic risk in South African gold mines.

We were very much encouraged to make additional plans to see more detailed of stress distribution of seismic sources in South African gold mines.

These measurements were funded by JST-JICA SATREPS and Anglogold Ashanti Ltd.

Photo. The M1.5 seismic damage at a pilot tunnel at 104L at Tau Tona, at the closest proximity of which the BX CCBO in-situ stress measurement was carried out. Harumi Kato and Gerhard Hofmann look at a potential rupture plane on the side wall. Photo by Hiroshi Ogasawara.

Keywords: In-situ stress measurement, Closest proximity of a hypocenter, South African gold mine, BX CCBO technique

SSS28-P20 Room:Convention Hall Time:May 23 18:15-19:30